Separation and Purification Technology 253 (2020) 117504

Contents lists available at ScienceDirect

Separation and Purification Technology

journal homepage: www.elsevier.com/locate/seppur

Description of the filter cloth deformation during backwashing filtration

Patrick Morsch*,[1], Maurus Bauer, Christoph Kessler, Harald Anlauf, Hermann Nirschl

Institute of Mechanical Process Engineering and Mechanics (MVM), Process Machines (VM), Karlsruhe Institute of Technology (KIT), Germany

ARTICLE INFO

Keywords:
Liquid filter cake discharge
Force-stretch behaviour of filter cloth
Backwashing filtration
Filter cloth deformation
Geometrical moment of inertia
Bulging-out behaviour
Register distance

ABSTRACT

The separation of fine particles with filter cloth is a commonly used technique to remove particles from process streams under low-cost and low-maintenance conditions. Such kind of filter apparatus can be found, i.e., in front of distillation columns with the adjusted size. Here, it is possible to have a filter apparatus with filter elements ≤ 2.5 m in length and ≤ 100 elements in one vessel. For a constant and stable process conditions, a periodical regeneration of the filter cloth is absolute required. One option for realizing this procedure is discharging the built-up filter cake in liquid phase (backwashing filtration). Due to the reverse flow, a deformation of the filter cloth occurs. This deformation depends on the assembly situation, mechanical pre-loading of the weave, the environment of the system, the weave type and, of course, the backwashing pressure. The interaction of this variables results in an adjusting of the space between the filter elements and correspond with the required backwashing volume in l/m^2.

Influence of a contact between two filter elements is not known but can have a negative impact in case of remaining filter cake on surface. Too much space reduces the economy of the apparatus because less filter surface needs the same apparatus footprint. Thus, by knowing how the filter cloth expand, the space can be adjusted on the particular separation task. This can lead to an improvement of the filter surface per apparatus footprint and can be advantageously compared to competing separations procedures. The deformation of the filter cloth during the backwashing treatment is described and discussed in the context of this investigation on the basis of elementary mechanics.

1. Introduction

The separation of particles by means of filter fabrics is a common method for removing particles from process streams in a cost-effective and low-maintenance manner. Such filter apparatuses can be found, for example, upstream of distillation columns and are correspondingly large (filter elements ≤ 2.5 m in length; up to 100 filter elements per apparatus). For constant and stable process control, it is essential to regenerate the filter after complete filtration [1]. One way of achieving this, is to carry out filtration with regular flow reversal (backwashing filtration) [2].

While the theory of filtration has been comprehensively analysed and documented, filter backwashing represents an inadequately investigated application. Knowledge of the theoretical principles of backwashing and the correct choice of cleaning parameters are important for the economical operation of a backwashing filter system.

Regeneration by backwashing results in bulging of the filter cloth due to flow reversal. This behavior has been studied for gas pulse-based cake discharge and depends on the backwashing pressure and the acceleration of the fabric acting on the cake [3,4]. This deformation depends, among other things, on the installation configuration, the pretension, operation conditions and the pressure acting on the weave.

Fig. 1 shows filter elements installed on one register. It becomes clear that the correct choice of the element distance is largely determined by the deformation of the fabric occurring during regeneration/backwashing. This process is shown schematically in Fig. 1(b) [5]. If the distance between the filter elements is too small, they obstruct each other during backwashing. Efficient cleaning is not to be expected here. If, on the other hand, the register distance and element distance is too large, good cleaning will take place, but the ratio of filter area to apparatus footprint is too small. Knowledge of the bulging behaviour is therefore necessary to optimize the regeneration and filter design economy.

One possibility to describe the deformation behaviour of filter fabrics is provided by the bending beam theory known from technical mechanics [6,7].

The present study assesses whether this theory is suitable for describing the deformation of fabric during backwash filtration. The aim

* Corresponding author.
E-mail address: patrick.morsch@kit.edu (P. Morsch).
[1] Research Fellow.

https://doi.org/10.1016/j.seppur.2020.117504
Received 11 December 2019; Received in revised form 29 July 2020; Accepted 29 July 2020
Available online 03 August 2020

Nomenclature

Symbols

E	Young modulus [N/mm^2]
H	Height variable [mm]
I(x)	Geometrical moment of inertia [mm^4]
l_{tot}	Total length of the filter [mm]
q_0	Line load [N/mm]
w(x)	Bulge [mm^4]
x	Length coordinate [mm]

the efficiency of the entire process suffers.

To prevent the filter regeneration from becoming the bottleneck of the filtration process, the present paper deals with the optimization of the spacing among filter elements and registers according to Fig. 1. The aim is to enable an increase of the filtration area by smaller element and register spacings and to achieve an improvement of the regeneration by backwashing.

3. Material and method

As already explained in Fig. 1, it is essential for optimal operation of a filter system to know the bulging of the filter used during regenera-

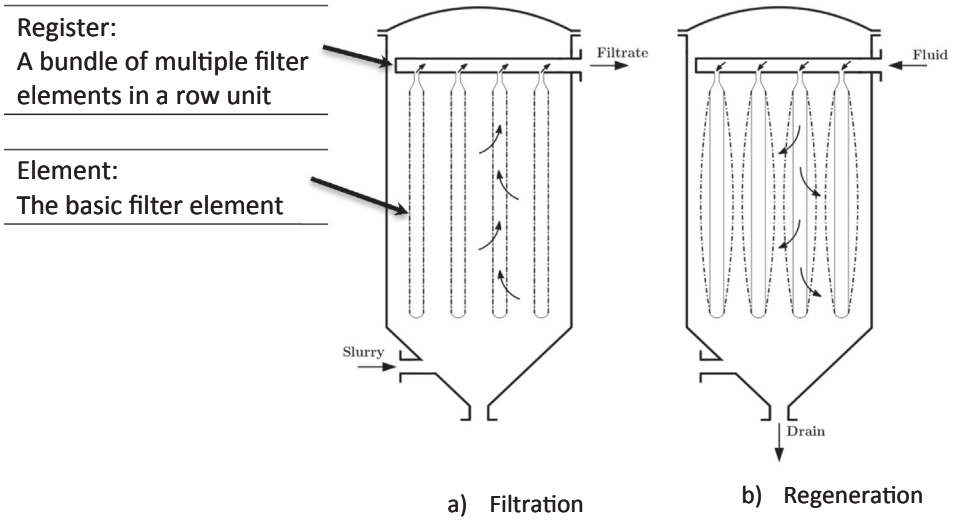

Fig. 1. Backwashing filter during filtration (a) and regeneration (b). The bulging of the filter cloth during backwashing is shown schematically [5].

is to enable an increase in the filter area per footprint based on an accurate description of the expansion behaviour of the filter cloths.

2. Mechanisms of filter cloth deformation

The mechanical behaviour of the filter cloth during regeneration by backwashing is already the subject of many publications in gas filtration and especially in bag filters [3,4,8,9]. In the case of liquid filtration, this process has only been studied for dry cake discharge with a gas backflow [10,11].

The process of liquid filtration in the liquid phase with subsequent cake discharge with a liquid backflow, although extensively practiced in the industry is only currently being investigated [2]. A theoretical description of the mechanical behaviour of filter cloths is completely unknown and is only described by assumed strains and their effects [11]. The filter cloth stretching has a significant influence on the regeneration with regard to the necessary backwashing volume.

Adequate understanding not only in gas backflow for dry cake discharge but also in liquid backflow mode wet cake discharge filtration is an essential step to design backwashing filters. Poor cleaning increases the pressure loss or reduces the available filter area, because of which tion. This is underlined, for example, by the fact that the bulging of the filter fabric increases the necessary backwash volume by 50–60%.

At present the choice of the register and element spacing is an in-house experience but is not based on knowledge of the mechanical behaviour of the filter cloth. In the context of this work the bulging behaviour of various filter fabrics caused by backwashing is therefore examined in more detail. The procedure of the investigation comprises three points:

- Selection of representative filter fabrics
- Determination of the mechanical properties of the fabrics (force-stretch behaviour)
- Flow through the fabric in a filter system and measure the bulge

After the selection of suitable filter fabrics, the force-stretch behaviour is evaluated. For this purpose, the fabrics are examined in a tensile testing machine. The aim here is to determine the bulging behaviour of the filter cloths used to understand the deformation occurring during backwashing on this basis. Filtration and backwashing then take place in a leaf filter system. Here, the filter fabric is flowed through and the bulge is evaluated by imaging. The selection of the filter fabrics,

Table 1
Overview of the filter fabrics used.

Fabric type/mesh size [µm] /Material			Weave type [DIN ISO 9354]	Weight per area [g/dm^2]	Surface roughness (ISO 25178)	Thread thickness warp/weft [µm]	Fabric thickness (ISO 5084) [µm]
twill	11	PET	20-03 01-01-03	2	29	132/429	245
	14	PP	20-02 01-01-02	1.25	40	168/161	200
	20	PET	20-03 01-01-03	2	30	128/160	260
plain reverse dutch	12	PET	10-01 01-01-00	0.5	9	100/45	80

as well as the structure of the corresponding tests and their execution are explained in the following chapters.

3.1. Filter fabrics

The basis for the examination are the fabrics listed in Table 1. The filter cloths vary in weave type and pattern in order to achieve a general validity of the measurements performed.

The three twill fabrics examined have mesh sizes of 11 µm, 14 µm and 20 µm. While the 14 µm twill fabric is made of polypropylene (PP), the other two are made of polyethylene terephthalate (PET). The used plain reverse dutch filter cloth also consists of PET and has a mesh size of 12 µm (see Table 1).

Looking at the weave pattern, the 11 µm and the 20 µm fabrics are similar. Here, three warp lifts are followed by a warp lowering. In the case of the 14 µm fabric, the weaving pattern is given by two warp thread transfers to a warp thread underpass. The plain reverse dutch weave shows the usual variation between warp lifting and warp lowering. All fabric types are monofilament in warp and weft direction and have a single-thread weaving pattern.

The number of offsets in the twill fabrics corresponds to the number of warp lifts, which means that there is no twill of the same degree, but an inclined or wide twill. Due to the type of weave, the weight per area of the twill fabrics is considerably greater than those of the plain reverse dutch fabric. Due to the thicker threads, the filter cloths with twill weave are rougher than the plain reverse dutch fabric, which is also noticeable in the overall thickness.

The filter cloths examined within the scope of this work thus show a clear variation in the following points:

- Weave type
- Mesh size
- Material
- Thread/weave thickness

With regards to twill and plain reverse dutch fabrics, this is therefore a representative selection for filter fabrics < 20 µm. Fabrics with satin weave are not included in this paper.

3.2. Experimental set-up – Tensile testing machine

The stress-strain behaviour of the fabrics is determined using a tensile testing machine. The test setup and execution are based on ASTM Standard 6614–07.

In order to install the fabric in the tensile testing machine, it is clamped in the device shown in Fig. 2(a). The filter frame used here has a width of 50 mm. The fabric is then stretched. The force applied by the pulling device and the corresponding change in length are detected. The measured change in length is related to the initial length of 150 mm (see Fig. 2(a)), resulting in the fabric elongation. The tension acting in the filter cloth is calculated from the recorded force using the fabric width (50 mm) and fabric thickness (see Table 1).

Thus it is possible to record the tension curve of the 11 µm twill fabric in warp direction as shown in Fig. 2b). The test moves completely in the elastic area of the fabric. Here it becomes clear that the stress can be divided into several areas (see Fig. 2b):

I. High elongation with low force
II. Exponential force increase with comparatively low elongation increase
III. Further increase in force at low elongation

Especially at the beginning of the tensile tests, significant changes in elongation at low force can be observed. If this range is linearized (coefficient of determination > 95%), a slope of ~85 N/mm^2 is recorded for strains of up to 0.4%. The gradient corresponds to the modulus of elasticity, modelled on Hook's range. With further elongation, the necessary force increases strongly. Here, for example, a modulus of elasticity of 1247.6 N/mm^2 can be determined for strains of 0.4 to 0.6% for the second range. An increase of the Young's modulus by a factor of fifteen can be explained by different physical processes in the fabric during elongation. While in the beginning (area I) the elongation is mainly caused by a displacement of the fabric meshes in the weaving pattern, in area II the elongation is mainly caused by direct tensile loading of the fibres. For this reason, a strong increase in the modulus of elasticity in the direction of the material characteristic value of PET (according to ISO 527–2 approx. 3600 N/mm^2) can be observed. With a further increase in force, the increase in elongation is less pronounced. Thus, a further increase of the Young's modulus to ~1800 N/mm^2 for elongations up to 1.07% can be observed.

After knowing of the stress-strain curve, the filter cloth is bulged on a leaf filter system. In this test, the fabric is deliberately used as a flat leaf filter to investigate the influence of warp and weft direction. Effects of a cylindrical shape of the filter cloth, as they occur with the widely

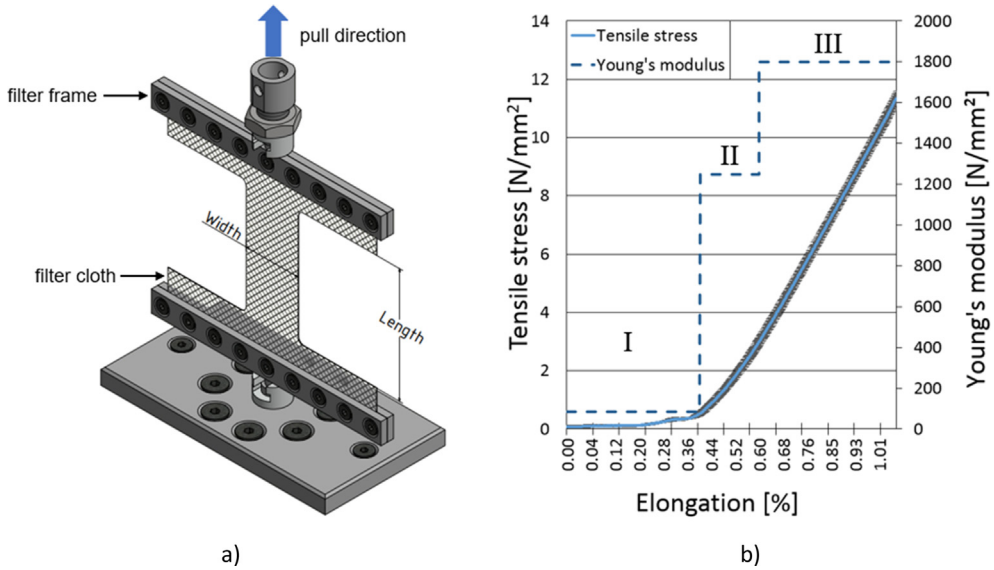

Fig. 2. Illustration of the test setup for determining the tensile strength of filter fabric (a) and exemplary illustration of the stress-strain diagram with linearization and modulus of elasticity for the 11 µm filter cloth in warp direction (b).

used candle filters, are not examined in detail in this paper. The structure and performance of the backwash tests are described in the following chapter.

3.3. Experimental set-up – Leaf filter

The bulge tests are carried out using a leaf filter with a filter area of 150 × 100 mm^2. Due to the rectangular filter profile, influences of the weaving direction on the fabric deformation can be illustrated. Fig. 3 shows the structure of the filter element. This consists of the actual leaf filter, which is loosely embedded in a stenter frame. If a fabric is mounted on the filter element, the fine thread can be used to move the leaf filter against the fabric. This creates a defined pre-tension of the fabric.

The bulging of the filter cloth occurs at defined pre-tensions of 1 Nm and 10 Nm for different backwash pressures (0.3/1.5/3.0 bar). The individual backwashing processes are recorded visually using a camera. The resulting bulging of the fabric is then determined by image evaluation.

Now that the stress-strain behaviour and the bulge are known, the geometrical moment of inertia I(x) of the filter cloth can be determined according to Eq. (1). The variable is a moment of resistance to bending, which originally comes from the bending beam theory of technical mechanics/statics. In the case of a bending beam clamped on both sides, the differential equation provides the form integrated in Eq. (1) [6,7]. It holds that the greater I(x), the more stable the body is against bending. When transferred to filter fabric, this is equivalent to bulging. This is because the fabric on the leaf filter is also a body clamped on both sides which is deformed with an even load. If the bulge w(x) is now resolved against the bulge, the equation shown in Eq. (2) results.

With the knowledge of I(x) it is then possible to calculate the bulge w(x) of a real backwash process (Eq. (2)). This allows the distance between the filter elements to be adjusted and the filter area utilization to be improved. Since the maximum bulging occurs in the middle of the filter cloth, only the length variable x must be replaced by ½ ·l_{tot}. The l_{tot} represents the total length of the fabric. The Young modulus must be adapted to the elongation, since fabrics exhibit anisotropic, nonlinear elongation behaviour (see Fig. 2(b)). The description of the individual variables and their origin are summarized under “Sources” in the description of the equation.

$$I(x) = \frac{\frac{1}{24}\cdot q_0\cdot x^4 - \frac{1}{12}\cdot q_0\cdot l_{tot}\cdot x^3 + \frac{1}{12}\cdot q_0\cdot l_{tot}^3\cdot x}{E\cdot w(x)} \quad (1)$$

$$w(x) = \frac{\frac{1}{24}\cdot q_0\cdot x^4 - \frac{1}{12}\cdot q_0\cdot l_{tot}\cdot x^3 + \frac{1}{12}\cdot q_0\cdot l_{tot}^3\cdot x}{E\cdot I(x)} \quad (2)$$

Symbol	Unit	Description	Source
q_0	[N/mm]	Line load	Measured and calculated
l_{tot}; x	[mm]	Length coordinate	Geometric dimension
w(x)	[mm]	Bulge	Optical measurement
E	[N/mm^2]	Young modulus	Stress–strain curve measurement
I(x)	[mm^4]	Geometrical moment of inertia	Calculated

4. Interpretation

The study carried out in the context of this work can be divided into the following key points:

I. Determination of fabric-dependent strength values
II. Determination of the filter bulge at the leaf filter
III. Calculation of the second moments of area of the fabrics

The following section describes the results of the tensile tests and the measured bulge during backwashing.

4.1. Tensile test and bulging

As shown in Fig. 2b), the areas for determining the Youngs moduli can generally be described by three envelopes. These are summarized in Table 2 for the four investigated filter cloths. The Youngs moduli in warp and weft direction of the fabrics are shown for different elongations, as well as the bulge during backwashing as a function of preload (expressed by torque) and backwash pressure (0.3–3.0 bar).

In the case of the 11 µm fabric, there is a strong increase in elongation in the warp direction with minimal effort (see area I in Fig. 2(b)). In this area, the meshes shift against each other. Then, in area II, the modulus of elasticity increases sharply to approx. 1250 N/mm^2. The modulus of elasticity reaches its maximum value in area III with a value of approx. 1800 N/mm^2 at an elongation of 1.07%. Here the fabric begins to deform plastically. In the case of the tensile tests in the weft direction. Here a significantly greater elongation (up to 1.5%) takes place at a lower stress (290 N/mm^2). The 12 µm weave also exhibits similar behavior, albeit to a lesser extent. Here a stress of ~1500 N/m^2 is measured at a maximum elongation of 1.14% in warp direction, while the modulus of elasticity at similar elongation in weft direction (1.17%) is only ~910 N/mm^2. In the case of the 14 µm twill fabric, the elongation range can be described with only two envelopes. Here a clear difference between warp (1% elongation with 1043 N/mm^2) and weft (3.8% elongation with 76 N/mm^2) is found. The 20 µm fabric behaves analogously to the 11 and 14 µm fabric. In total, however, a clearly anisotropic behaviour of the fabrics can be observed.

With regards to deformation, the expected trend that increasing prestressing will reduce bulging is confirmed. The bulge furthermore increases with rising backwashing pressure.

However, special features can also be observed. In the case of the 11 µm fabric in warp direction, the bulge is similar at backwash pressures of 3.0 bar in the case of a preload of 1 Nm and 10 Nm. Here it can be expected that the fabric will be moved from the elastic to the plastic area by the high load. A permanent change in length with the associated change in elongation is to be expected. The situation is similar at 11 µm in the weft direction. Here even a larger bulge is measured at higher preload. Similar behaviour can also be observed at 12 µm in the weft direction and at 14 µm in the warp direction. Here the added value for practice is, that a too high pre-tension of the fabric is

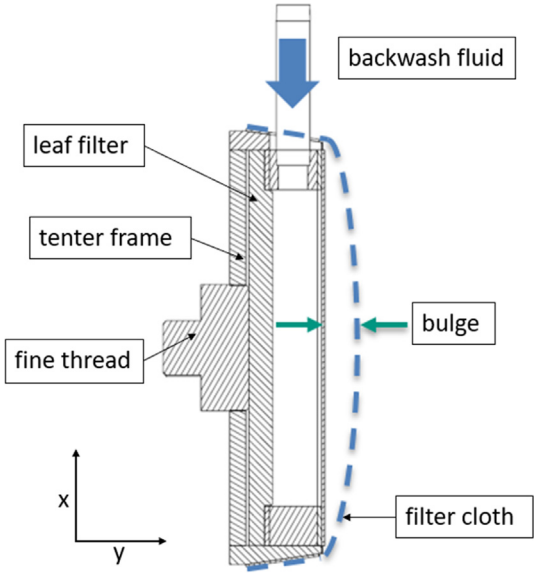

Fig. 3. Sectional view of the leaf filter in the stenter frame with exemplary depicted bulging of the fabric (dashed line) during backwashing procedure.

Table 2
Young moduli and bulges for the four investigated filter fabrics.

Fabric		Young Modulus for defined elongation ranges ε [N/mm²]			Preload torque	Bulge		
		Area I	Area II	Area III	[Nm]	[mm]		
Fabric type	thread direction				Backwash pressure →	0.3 bar	1.5 bar	3.0 bar
11 µm	warp	0% ≤ ε < 0.40%	0.40% ≤ ε < 0.60%	0.60% ≤ ε < 1.07%	1	11.3	16.4	18.1
20-03 01-01-02		**84.98**	**1247.60**	**1798.55**	10	9.4	15.5	17.7
	weft	0% ≤ ε < 0.41%	0.41% ≤ ε < 0.69%	0.60% ≤ ε < 1.52%	1	9.5	10.9	11.9
		77.77	**109.60**	**290.64**	10	8.7	10.5	12.1
12 µm	warp	0% ≤ ε < 0.50%	0.50% ≤ ε < 0.80%	0.80% ≤ ε < 1.14%	1	13.9	16.1	17.6
10-01 01-01-00		**225.98**	**881.93**	**1487.15**	10	8.0	11.8	14.0
	weft	0% ≤ ε < 0.39%	0.39% ≤ ε < 0.65%	0.65% ≤ ε < 1.17%	1	13.8	14.9	15.6
		236.63	**702.64**	**912.62**	10	15.6	16.7	17.5
14 µm	warp	0% ≤ ε < 0.15%	0.15% ≤ ε < 1.03%	-	1	17.5	18.5	19.1
20-02 01-01-02		**457.08**	**1043.39**	-	10	16.8	18.6	19.1
	weft	0% ≤ ε < 0.33%	0.33% ≤ ε < 0.66%	0.66% ≤ ε < 3.79%	1	14.9	16.1	16.6
		88.39	**30.02**	**76.76**	10	10.7	11.8	12.3
20 µm	warp	0% ≤ ε < 0.35%	0.35% ≤ ε < 0.50%	0.50% ≤ ε < 0.76%	1	16.3	17.9	18.6
20-03 01-01-03		**130.07**	**1378.11**	**2025.31**	10	3.0	5.0	6.0
	weft	0% ≤ ε < 0.33%	0.33% ≤ ε < 0.73%	0.73% ≤ ε < 0.91%	1	10.0	10.9	11.5
		105.90	**468.38**	**565.19**	10	2.7	4.7	5.8

counterproductive for backwash filtration.

Another remarkable observation is, that the weft direction has a smaller bulge than the warp direction. This becomes clear with the 20 µm twill fabric. Although the modulus of elasticity in the warp direction is higher and therefore requires more force per stretch, the bulge for warp direction on the long edge (150 mm) of the filter fabric is greater. This is based on the superposition principle. Under the assumption that the more stable fibre direction determines the bulging, in the case of the warp direction on the 150 mm side of the leaf filter the fabric fibres have a greater possibility of elongation than would be the case with the 100 mm side (load in the weft direction). This behaviour can also be observed for all other fabrics. The added value for practice here is that the fabric fibre with the higher strength should be mounted on the shorter side of right-angled filter elements in order to achieve the lowest possible bulging. In summary, the following findings can be taken from Table 2:

- Anisotropic behaviour of the filter fabrics
- Reduced bulging with stiffer fabric
- Greater bulging when fiber with lower strength is on long filter edge
- Deviations from standard behaviour with larger preloads/backwash pressures

4.2. Geometrical moment of inertia

After the first step in the geometrical determination of strain behavior and bulging, the geometrical moment of inertia (cf. Eq. (1)) are calculated for the different preloads and backwashing pressures. For this purpose, the backwashing pressure in N/mm² is converted into a line load in N/mm with the geometry of the filter cloth and the moment of inertia is calculated with the aid of the cloth length l_{tot} and the point of maximum cloth bulge $x = ½ \cdot l_{tot}$, the modulus of elasticity E(ε) and the measured bulge w(x) at the point $x = ½ \cdot l_{tot}$.

These are summarized in Table 3 as mean geometrical moment of inertia over the entire range of backwash pressures (0.3, 1.5, and 3.0 bar). This is possible with regards to Eq. (1), since in the case of a higher backwash pressure the bulge also increases. Only the modulus of elasticity increases as a result of the larger bulging and would have to be iteratively adapted to the strain, for example for a simulation.

The connection of the elongation ε as a function of the modulus of elasticity is (ε = f(E)), because it applies equally to the modulus of elasticity, which increases with increasing elongation (E = f(ε)). Taking Table 3 into account, it is noticeable that the second moment of area for all fabrics ranges from 10^5 - 10^6 mm⁴ for fabrics < 20 µm, backwash pressures from 0.3 − 3.0 bar and prestressing torques of 1 and 10 Nm. It should be noted that fabrics with lower bulging have a higher modulus of elasticity and the fluctuation of the geometrical moment of inertia, analogous to the bulge, is lower. According to [2], the required backwash volume for cake discharge by liquid backwashing is not pressure-dependent. Only the cake discharge process is accelerated with higher backwashing pressure. From this point of view, smaller backwashing pressures can be selected so that the bulge and thus the geometrical moment of inertia required for the design is smaller (0.3 bar: 4.5·104 to 105). Based on this knowledge, the real bulge can be estimated with a geometrical moment of inertia of 10^5–10^6 mm⁴. For a conservative design, a smaller geometrical moment of inertia must be used so that the bulge is assumed to be larger. The design of the element distances is then based on Fig. 1 as the sum of the double bulge, the double filter

Table 3
Average Geometrical moment of inertia over all backwash pressures 0.3-3.0 bar) and preload torques (1-10 Nm).

Fabric type/mash size [µm]/Material			Weave type [DIN ISO 9354]	Geometrical moment of inertia [mm⁴]
Twill	11	PET	20-03 01-01-03	warp: $3.04 \cdot 10^5 \pm 2.80 \cdot 10^5$ weft: $3.52 \cdot 10^6 \pm 2.45 \cdot 10^6$
	14	PP	20-02 01-01-02	warp: $3.13 \cdot 10^6 \pm 2.12 \cdot 10^6$ weft: $4.37 \cdot 10^6 \pm 2.85 \cdot 10^6$
	20	PET	20-03 01-01-03	warp: $2.85 \cdot 10^5 \pm 8.18 \cdot 10^4$ weft: $2.87 \cdot 10^5 \pm 2.34 \cdot 10^5$
Plain reverse dutch	12	PET	10-01 01-01-00	warp: $2.85 \cdot 10^5 \pm 8.18 \cdot 10^4$ weft: $2.87 \cdot 10^5 \pm 2.34 \cdot 10^5$

cake thickness and a safety factor and is shown in Eq. (3).

$$H_{Element} = 2 \cdot H_{Bulge} + 2 \cdot H_{filter\ \ cake\ \ thickness} + H_{Safety} \quad (3)$$

The Geometrical moment of inertia resolved for the respective pressure and calculated with the bulge from Table 2 is broken down in Table 4. The example of the 11 µm twill fabric illustrates why the standard deviations in Table 3 are sometimes of similar magnitude to the mean value. Here, for a backwash pressure of 0.3 bar, the calculated geometrical moment of inertia for 11.3 mm bulge (warp direction) has the value $5.64 \cdot 10^4$ mm^4 and increases with increasing backwash pressure to $1.34 \cdot 10^5$ mm4 (1.5 bar) and $2.44 \cdot 10^5$ mm^4 (3.0 bar). In the weft direction, the increase is less pronounced, but the geometrical moment of inertia of 10^6 mm^4 is one order of magnitude greater. The reason for this has already been discussed and is that in the case of "weft direction on long filter element edge" the more stable warp threads lie on the shorter fabric edge. The validity of the superposition principle becomes clear here based on the larger geometrical moment of inertia or the smaller bulge.

Also, the 12 µm weave follows this tendency, whereby for each combination of backwash pressure and preload an increase of one variable is accompanied by an increase of the geometrical moment of inertia. Only at a preload of 10 Nm from 1.5 bar to 3.0 bar the geometrical moment of inertia stagnates due to a plastic deformation of the filigree plain reverse dutch weave due to the slight increase of the bulge and at the same time a strong increase of the geometrical moment of inertia (see Table 2).

This tendency is also confirmed for the 14 µm and 20 µm twill fabric without outliers. Both fabrics even have the highest geometrical moment of inertia in the 10^7 mm^4 range in the weft direction. Only the 14 µm fabric shows an abnormality in the warp direction when compared with 1 Nm and 10 Nm pre-tension. The geometrical moment of inertia shows similar values here. This is due to the constant gradient of the modulus of elasticity of 1043.39 N/mm^2 even at slight elongations of > 0.15%.

In summary, because of their anisotropic force-stretch behaviour, the fabrics do not exhibit any linear stretching during backwashing. However, the description geometrical moment of inertia for different strains is possible and provides values in the range 10^4–10^7 mm^4. The values for lower backwash pressures (0.3 bar; tendency towards 104 mm4) are to be classified as technically relevant. The more stable fibre direction should also be clamped on the shorter edge of the filter geometry.

5. Conclusion

The results of this study show that the Young moduli of filter fabrics exhibit highly anisotropic behaviour. Nevertheless, they can be used to predict strain in backwash filters.

This shows that particularly stiff fabrics have low bulges. This leads to a lower backwashing volume until the fabric is regenerated and smaller possible element distances between the elements.

Furthermore, the more stable weaving direction (warp or weft) for rectangular fabrics must be stretched onto the shorter edge of the filter element. This allows the fabric to expand less, as the more stable thread direction is the deformation determining side. The element distances are reduced.

A certain pre-tension of the fabric also leads to a further reduction in bulging. Alternatives are support grids on the filtrate side. In this case, however, the support grid reduces the free filter area, which is accompanied by a reduction in the filter capacity. Negative effects on the regeneration can only be assumed here (e.g. "interlocking" of the filter cake on the supporting fabric).

Since the strain was known in the previous determination of the second moments of area and the modulus of elasticity could be adapted to it, real designs in the vessel must react to this design by iterative adaptation of the modulus of elasticity. A conservative design in the form of an additional "safety distance" is recommended here. A similar procedure is known in the technical field, e.g. for the design of pressure vessels.

The second moments of area are similar in their tendency (10^4–10^5 mm^4, partly 10^6–10^7 mm^4 for small bulges) for all investigated fabrics (mesh size < 20 µm). Here, the smaller value should be used for a more conservative design. This means that the calculated bulge is assumed to be greater according to Eqs. (1) and (2). It is therefore possible to estimate the bulge.

Table 4
Geometrical moment of inertia based on the bulge from Table 2 over all backwashing pressures (0.3–3.0 bar) and prestressing torques (1–10 Nm) for the four investigated fabrics.

Fabric type/mash size[µm]		Weave type [DIN ISO 9354]	Pressure [bar]	Geometrical moment of inertia 1 Nm pretension [mm^4]	Geometrical moment of inertia 10 Nm pretension [mm^4]
Twill	11	20-03 01-01-03	0.3	warp – 1 Nm: $5.64 \cdot 10^4$ weft – 1 Nm: $1.08 \cdot 10^6$	warp – 10 Nm: $9.98 \cdot 10^5$ weft – 10 Nm: $3.46 \cdot 10^6$
			1.5	warp – 1 Nm: $1.34 \cdot 10^5$ weft – 1 Nm: $3.33 \cdot 10^6$	warp – 10 Nm: $1.42 \cdot 10^5$ weft – 10 Nm: $2.49 \cdot 10^6$
			3.0	warp – 1 Nm: $2.44 \cdot 10^5$ weft – 1 Nm: $6.07 \cdot 10^6$	warp – 10 Nm: $2.49 \cdot 10^5$ weft – 10 Nm: $5.98 \cdot 10^6$
	14	20-02 01-01-02	0.3	warp – 1 Nm: $4.36 \cdot 10^4$ weft – 1 Nm: $6.95 \cdot 10^5$	warp – 10 Nm: $4.53 \cdot 10^4$ weft – 10 Nm: $2.47 \cdot 10^6$
			1.5	warp – 1 Nm: $2.05 \cdot 10^5$ weft – 1 Nm: $3.20 \cdot 10^6$	warp – 10 Nm: $2.05 \cdot 10^5$ weft – 10 Nm: $1.12 \cdot 10^7$
			3.0	warp – 1 Nm: $3.99 \cdot 10^5$ weft – 1 Nm: $6.22 \cdot 10^6$	warp – 10 Nm: $3.99 \cdot 10^5$ weft – 10 Nm: $2.15 \cdot 10^7$
	20	20-03 01-01-03	0.3	warp – 1 Nm: $2.40 \cdot 10^4$ weft – 1 Nm: $1.69 \cdot 10^5$	warp – 10 Nm: $2.01 \cdot 10^6$ weft – 10 Nm: $2.82 \cdot 10^6$
			1.5	warp – 1 Nm: $1.10 \cdot 10^5$ weft – 1 Nm: $7.75 \cdot 10^5$	warp – 10 Nm: $6.12 \cdot 10^6$ weft – 10 Nm: $8.06 \cdot 10^6$
			3.0	warp – 1 Nm: $2.11 \cdot 10^5$ weft – 1 Nm: $1.48 \cdot 10^6$	warp – 10 Nm: $1.03 \cdot 10^7$ weft – 10 Nm: $1.29 \cdot 10^7$
Plain reverse dutch	12	10-01 01-01-00	0.3	warp – 1 Nm: $3.83 \cdot 10^4$ weft – 1 Nm: $6.31 \cdot 10^4$	warp – 10 Nm: $4.37 \cdot 10^5$ weft – 10 Nm: $5.59 \cdot 10^4$
			1.5	warp – 1 Nm: $1.66 \cdot 10^5$ weft – 1 Nm: $2.92 \cdot 10^5$	warp – 10 Nm: $3.83 \cdot 10^5$ weft – 10 Nm: $2.60 \cdot 10^5$
			3.0	warp – 1 Nm: $3.02 \cdot 10^5$ weft – 1 Nm: $5.56 \cdot 10^5$	warp – 10 Nm: $3.81 \cdot 10^5$ weft – 10 Nm: $4.97 \cdot 10^5$

CRediT authorship contribution statement

Patrick Morsch: Conceptualization, Methodology, Software, Formal analysis, Investigation, Validation, Resources, Writing - original draft, Project administration. **Maurus Bauer:** Investigation, Writing - review & editing. **Christoph Kessler:** Investigation, Writing - review & editing. **Harald Anlauf:** Supervision, Writing - review & editing, Funding acquisition. **Hermann Nirschl:** Supervision, Writing - review & editing, Funding acquisition.

Declaration of Competing Interest

The authors declare that they have no known competing financial interests or personal relationships that could have appeared to influence the work reported in this paper.

Acknowledgement

The authors would like to thank the German Federation of Industrial Research Associations (AiF) for the financial support (IGF number 18591N). The authors would also like to thank all colleagues and students for the support in writing this paper. Special thanks go to my student Mr. Simon Egner for the support during their time at the institute.

References

[1] A.J. Charleton, N.I. Heywood, Filtr. Sep. 20 (5) (1983).
[2] P. Morsch, P. Ginisty, H. Anlauf, H. Nirschl, Chem. Eng. Sci. (2019).
[3] J. Sievert, F. Löffler, Chem. Eng. Process. Process Intensif. 26 (1989) 2.
[4] J. Sievert, F. Löffler, Filtr. Sep. 24 (1987) 2.
[5] Gaudrin, Filters Gaudrin: worldpatents (1973).
[6] D. Gross, W. Hauger, J. Schröder, W. A. Wall, and J. Bonet, Engineering Mechanics 2: Mechanics of Materials (Springer Berlin Heidelberg, Berlin, Heidelberg, 2018) [eng].
[7] D. Gross, W. Hauger, J. Schröder, W. A. Wall, and N. Rajapakse, Springer textbook: Engineering Mechanics 1: Statics (Springer, Berlin, Heidelberg, 2013) [eng].
[8] M. Ferer, D.H. Smith, J. Appl. Phys. 81 (1997) 4.
[9] A. Dittler, M.V. Ferer, P. Mathur, P. Djuranovic, G. Kasper, D.H. Smith, Powder Technol. 124 (2002) 1–2.
[10] H.R. Muller, R. Kern, W. Stahl, Filtr. Sep. 24 (1) (1987).
[11] R. Kern, Die Optimierung des Kuchenabwurfs beim Scheibenfilter: Eine Voraussetzung für dessen Weiterentwicklung [ger].